

# Chlorophyll breakdown: Pheophorbide *a* oxygenase is a Rieske-type iron–sulfur protein, encoded by the *accelerated cell death 1* gene

Adriana Pružinská\*, Gaby Tanner\*, Iwona Anders\*, Maria Roca†, and Stefan Hörtensteiner\*\*

\*Institute of Plant Sciences, University of Bern, Altenbergrain 21, CH-3013 Bern, Switzerland; and †Plant Genetics and Breeding Department, Institute of Grassland and Environmental Research, Plas Gogerddan, Aberystwyth, Ceredigion SY23 3EB, United Kingdom

Communicated by J. Clark Lagarias, University of California, Davis, CA, October 10, 2003 (received for review August 27, 2003)

Chlorophyll (chl) breakdown during senescence is an integral part of plant development and leads to the accumulation of colorless catabolites. The loss of green pigment is due to an oxygenolytic opening of the porphyrin macrocycle of pheophorbide (pheide) *a* followed by a reduction to yield a fluorescent chl catabolite. This step is comprised of the interaction of two enzymes, pheide *a* oxygenase (PaO) and red chl catabolite reductase. PaO activity is found only during senescence, hence PaO seems to be a key regulator of chl catabolism. Whereas red chl catabolite reductase has been cloned, the nature of PaO has remained elusive. Here we report on the identification of the PaO gene of *Arabidopsis thaliana* (*AtPaO*). *AtPaO* is a Rieske-type iron–sulfur cluster-containing enzyme that is identical to *Arabidopsis* accelerated cell death 1 and homologous to lethal leaf spot 1 (LLS1) of maize. Biochemical properties of recombinant *AtPaO* were identical to PaO isolated from a natural source. Production of fluorescent chl catabolite-1 required ferredoxin as an electron source and both substrates, pheide *a* and molecular oxygen. By using a maize *lls1* mutant, the *in vivo* function of PaO, i.e., degradation of pheide *a* during senescence, could be confirmed. Thus, *lls1* leaves stayed green during dark incubation and accumulated pheide *a* that caused a light-dependent lesion mimic phenotype. Whereas proteins were degraded similarly in wild type and *lls1*, a chl-binding protein was selectively retained in the mutant. *PaO* expression correlated positively with senescence, but the enzyme appeared to be post-translationally regulated as well.

During leaf senescence, chlorophyll (chl) is degraded to colorless linear tetrapyrroles, termed nonfluorescent chl catabolites (NCCs; refs. 1–3). The pathway of chl catabolism (Fig. 1A) includes the occurrence of both colored and colorless intermediates. Thus, in two subsequent reactions catalyzed by chlorophyllase and Mg dechelataase, respectively, phytol and the central Mg atom are removed. Then, the ring structure of pheophorbide (pheide) *a* (Fig. 1A) is oxygenolytically opened at the  $\alpha$ -mesoposition between C4 and C5 by pheide *a* oxygenase (PaO). The product, red chl catabolite (RCC), does not accumulate *in vivo* (4) but is rapidly converted to a primary fluorescent chl catabolite (pFCC) by a stereospecific reduction of the C20/C1 double bond. The source of the responsible enzyme, RCC reductase (RCCR), defines which of two possible C1 isomers, pFCC-1 or -2, occurs (Fig. 1A). RCCR of *Arabidopsis* has been shown to produce pFCC-1 (5). Further steps of the chl breakdown pathway involve reactions known from plant detoxification mechanisms (6). FCCs are hydroxylated and in some cases conjugated with a glucosyl or malonyl moiety (7, 8), followed by their export into the vacuole by a primary active ATPase (9). Finally, FCCs are nonenzymically tautomerized to the respective NCCs because of the acidic pH inside the vacuole (10).

The biochemistry of chl catabolism has been investigated extensively during the last years (for recent reviews, see refs. 3, 5, 11, and 12). Surprisingly, PaO turned out to be a key regulator of this pathway. Thus, PaO activity is detectable only during

senescence (13, 14), whereas activities of other enzymes, such as chlorophyllase and RCCR, are constitutive (15–17). In addition, the reactions catalyzed by PaO and RCCR are responsible for the loss of pigment color. Biochemical evidence suggests that the two enzymes are interacting during catalysis. Thus *in vitro*, the intermediate, RCC, does not accumulate to substantial amounts in the absence of RCCR, indicating that RCC is metabolically channeled (4). PaO has been demonstrated to be located at the inner envelope of senescing chloroplasts (18). In contrast, RCCR is a stroma protein, suggesting that pheide *a* to pFCC conversion occurs at the stromal periphery of the inner envelope (4, 19). The recent cloning of RCCR (20) has uncovered a distinct relationship to other plant bilin reductases, all of which are ferredoxin (Fd)-dependent (21). Reduced Fd is also needed as a source of electrons for the PaO/RCCR-catalyzed reaction (13, 19). PaO is a nonheme iron type (14) monooxygenase that introduces one atom of molecular oxygen at the  $\alpha$ -methine bridge of pheide *a* (Fig. 1A), giving rise to the formyl group attached to pyrrole ring B in pFCC (22). Its activity is restricted to pheide *a*, with pheide *b* being a competitive inhibitor. Consequently, all NCCs identified so far are derived from chl *a* (23). Before entering this degradation pathway, chl *b* has to be converted to chl *a*. A respective chlorophyll cycle that is responsible for the interconversion of both types of chl has been described (24, 25). In addition, activity of one of the enzymes involved in chl *b* to *a* conversion, chl *b* reductase, increases during barley leaf senescence (26).

Senescence is the final stage of leaf development, ultimately leading to the death of the entire leaf. It is a highly regulated process that involves an ordered disintegration of chloroplast components, such as thylakoid membranes, along with the remobilization of amino acids from proteins, such as the chl *a/b*-binding proteins, and the subsequent release of potentially phototoxic chl. It is commonly believed that the function of chl degradation in plants is to avoid this hazard (3). chl in its free form would cause photooxidative damage to the senescing cell, and it has been shown that the accumulation of photoactive intermediates of chl biosynthesis causes a premature cell death phenotype in two chl biosynthetic mutants and transgenic plants (27, 28). This is termed a lesion mimic phenotype that, in contrast to the phenotypically similar hypersensitive response, occurs in the absence of pathogen infection. In addition to chl biosynthetic mutants, *Arabidopsis accelerated cell death 2* (*acd2*) has been isolated that develops a light-dependent lesion mimic phenotype (29). *acd2* is deficient in RCCR, and the phenotype has been suggested to be caused by the accumulation of phototoxic RCC (30). Thus, the ability of plants to degrade chl during

Abbreviations: chl, chlorophyll; FCC, fluorescent chl catabolite; pFCC, primary FCC; pheide, pheophorbide; PaO, pheide *a* oxygenase; RCC, red chl catabolite; RCCR, RCC reductase; NCC, non-FCC; Fd, ferredoxin.

†To whom correspondence should be addressed. E-mail: shorten@ips.unibe.ch.

© 2003 by The National Academy of Sciences of the USA

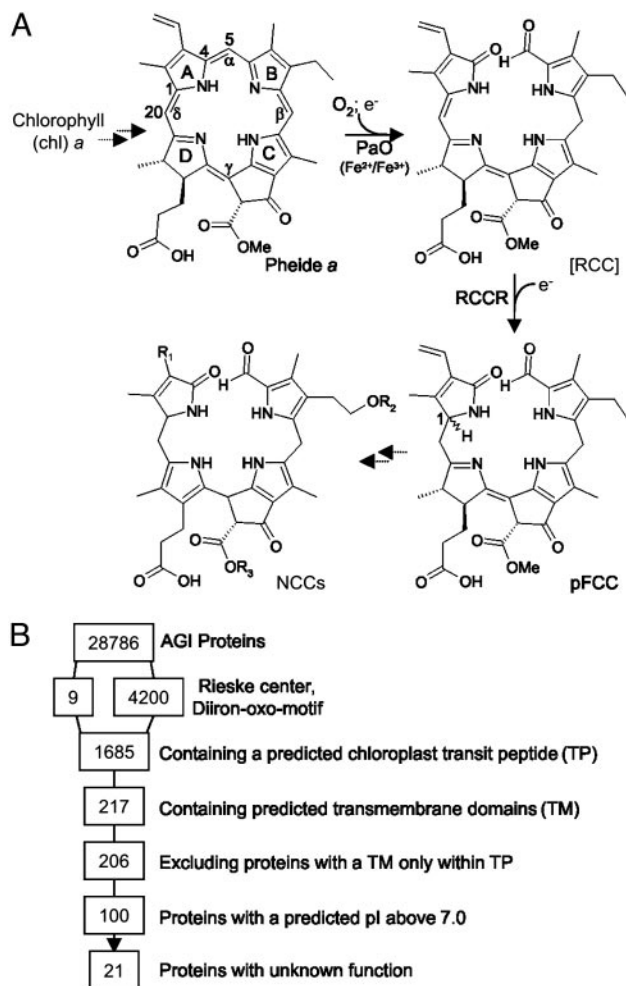


**Fig. 1.** The pathway of chl catabolism, and identification of possible PaO proteins in *A. thaliana*. (A) The pathway of chl catabolism. The key reaction is catalyzed by the joint action of PaO and RCCR. Chemical constitutions of chl catabolites are shown. Pyrrole rings (A–D), methine bridges ( $\alpha$ – $\delta$ ), and relevant carbon atoms are labeled. NCCs are species-specifically modified at different side positions ( $R_1$ – $R_3$ ). (B) Screening of the ATH1.pep database of the *Arabidopsis* Genome Initiative (AGI Proteins) for proteins with known properties of PaO.

senescence seems vitally important. Here we describe the molecular identification of PaO. In addition, we show that a mutant that is defective in PaO shows a stay-green phenotype in the dark and accumulates pheide *a*, which causes light-dependent premature cell death.

## Materials and Methods

**Plants and Growth Conditions.** The maize *lls1* mutant, containing the reference allele, was obtained from the Maize Genetics Cooperation Stock Center, University of Illinois at Urbana-Champaign, and was grown for 7–9 wk in a greenhouse. *Arabidopsis thaliana* ecotype Columbia was grown in soil under short-day conditions at  $120 \mu\text{mol}\cdot\text{m}^{-2}\cdot\text{s}^{-1}$ . For dark induction of senescence, excised *Arabidopsis* leaves or *lls1* leaf discs (1.0-cm diameter) were incubated on moistened filter paper or floating on tap water for several days, as indicated in Figs. 3–5.

**Computational Analysis.** The BULK PROTEIN ANALYSIS tool at The *Arabidopsis* Information Resource (TAIR; [www.arabidopsis.org](http://www.arabidopsis.org)) was used to screen the ATH1.pep database (Ver. 4.0) of the *Arabidopsis* Genome Initiative (31) for the presence of the

Rieske motif (PF00350). Proteins containing a diiron-oxo motif (32) were identified with the PATMATCH tool at TAIR. By using the BULK PROTEIN ANALYSIS tool (TAIR), a subset of 4,209 proteins was analyzed for the following properties: (i) proteins containing a putative plastid-targeting sequence (cTP), (ii) proteins containing putative transmembrane domains (TM), and (iii) prediction of pI. Proteins containing a TM domain only within the predicted cTP were eliminated manually. Screening for known protein function was done with the GENE ONTOLOGY and GENE HUNTER tools at TAIR.

**Analysis of Recombinant PaO.** Full-length cDNA clones of *Acd1* (pda07874) and At4g25650 (pda06002) were obtained from the RIKEN Tsukuba Institute BioResourceCenter (33). For subcloning into pQE30 (Qiagen, Chatsworth, CA), convenient restriction sites were introduced at the ends of the ORFs by PCR. After confirmation by sequencing, the respective constructs were expressed in *Escherichia coli* strains JM109 and C43 according to standard procedures. Total proteins were extracted as described (20), except that after sonication, extracts were treated with 2% (vol/vol) Triton X-100 (14) to solubilize membrane proteins. After the addition of 10% (vol/vol) glycerol, extracts were frozen in liquid nitrogen and stored at  $-80^\circ\text{C}$  until use. Expression of proteins was analyzed with immunoblots by using a RGS-His antibody (Qiagen).

**PaO Assays.** PaO activity was assessed by using a coupled PaO/RCCR assay according to established protocols (4, 14, 20). Briefly, the assay contained, in a total volume of 50  $\mu\text{l}$ , PaO, RCCR, and the following supplements: 2 mM pheide *a* (isolated according to ref. 20); 10  $\mu\text{g}$  of Fd (Sigma) and a Fd-reducing system [2 mM glucose-6-phosphate; 1 mM NADPH; 50 milliunits of glucose-6-phosphate dehydrogenase; 10 milliunits of Fd-NADPH-oxidoreductase (Sigma)]. As a source of PaO, either *E. coli* protein extracts (see above) or chloroplast membranes isolated from maize, *A. thaliana*, or oilseed rape (14) were used. As a source of RCCR, *Arabidopsis* RCCR expressed in *E. coli* was used (20). The production of pFCC-1 from pheide *a* was linear for >1 h of incubation at  $24^\circ\text{C}$  and was followed by reversed-phase HPLC (4, 20) by using 40 mM potassium phosphate, pH 7.0/methanol (2:3, vol/vol) as solvent. pFCC-1 eluting after  $\approx 8.0$  min under these conditions was quantified as integrated fluorescence units (14). Calculation of the apparent  $K_m$  was performed according to Lineweaver and Burk (34).

**Analysis of chl and chl Catabolites.** chl and polar green chl catabolites (pheides and chlorophyllides) were extracted from leaf tissues and separated by reversed-phase HPLC (35). For extraction of NCCs, maize leaf material (eight leaf discs) was homogenized in liquid nitrogen and extracted into 0.4 ml 0.1 M Tris-HCl, pH 8.0/methanol (1:4, vol/vol). After centrifugation, the supernatant was analyzed by HPLC (36). NCCs were eluted with a linear gradient of solvent B (20% (vol/vol) 25 mM potassium phosphate buffer, pH 7.0, and 80% methanol) in solvent A (50 mM potassium phosphate, pH 7.0) as follows: 0% to 100% over 15 min and 100% solvent B for 8 min. All pigments were identified by their absorption spectra and, in addition, green pigments were identified and quantified by using authentic standards (14, 36). chl was determined as described (37).

**RNA Isolation and RT-PCR.** RNA was prepared by using the Plant RNeasy Kit (Qiagen). After digestion of DNA with RQ1 RNase-free DNase (Promega), 1  $\mu\text{g}$  of RNA was reverse-transcribed with the RETROscript Kit (Ambion, Austin, TX). By using the QuantiTect SYBR Green PCR Kit (Qiagen), quantitative PCR was performed with a LightCycler according to the manufacturer's suggestions (Roche Diagnostics, Rotzrenz, Switzerland). Alternatively, relative RT-PCR analysis was performed accord-

**Table 1. List of 21 PaO candidates in the *Arabidopsis* genome**

Locus	$M_r$	pI	TM	AtDB annotation
At1g05750	55,761	8.40	2	Pentatricopeptide repeat-containing protein
At1g11470	16,268	9.61	1	Hypothetical protein
At1g48880	55,063	8.47	1	Hypothetical protein
At1g54320	38,937	10.00	2	Membrane protein common family
At1g67390	54,457	8.81	1	Hypothetical protein
At1g79760	33,653	9.00	2	Expressed protein
At2g07370	62,077	9.38	3	Hypothetical protein
At2g26920	71,040	7.28	1	Expressed protein
At2g40390	56,848	8.79	2	Expressed protein
At2g45870	46,262	8.83	1	Expressed protein
At3g02430	24,052	7.45	4	Hypothetical protein
At3g27180	56,369	9.34	2	Expressed protein
At3g44880	60,738	7.54	2	Rieske [2Fe-2S] domain-containing protein similar to lethal leaf-spot 1 from <i>Zea mays</i>
At3g61320	46,522	8.11	2	Expressed protein hypothetical protein
At4g24860	62,210	7.08	1	Hypothetical protein
At4g25650	63,801	8.81	2	Rieske [2Fe-2S] domain-containing protein similar to cell death suppressor protein <i>lls1</i> from <i>Z. mays</i>
At5g27010	98,190	8.58	1	Hypothetical protein, predicted proteins
At5g35570	72,893	7.26	1	Auxin-independent growth promoter-related protein
At5g42660	53,044	10.07	1	Expressed protein
At5g63390	62,873	10.30	2	Auxin-independent growth promoter-related protein
At5g64710	94,038	8.28	1	Expressed protein

Included are the names of the respective loci; their predicted molecular weight ( $M_r$ ), pI, and number of TM domains, respectively; and their annotation in the *A. thaliana* database. TM, transmembrane domain.

ing to the manufacturer's protocols (Ambion). Specific primers to the following genes were used: *Arabidopsis ACT2* (GenBank accession no. U41998: forward, 5'-TGGAATCCACGAGACAACCTA-3'; reverse, 5'-TTCTGTGAACGATTCCTGGAC-3'); *Sag12* (GenBank accession no. U37336: forward, 5'-CGAAGGCGGTTTAATGGATA-3'; reverse, 5'-CACCTCCTTC-AATTCCAACG-3'); *Acd1* (GenBank accession no. NM114357: forward, 5'-ACGGCATGGTAAGAGTCAGC-3'; reverse, 5'-AAACCAGCAAGAACCAGTCG-3'); maize *MubG1* (GenBank accession no. U29159: forward, 5'-GACCCTGACTGGAAAAACCA-3'; reverse, 5'-ACATCG-GCAGCTTAAACGAC-3'); *Lls1* (GenBank accession no. U77346: forward, 5'-TCGTTGAAATGCTCGTCTTG-3'; reverse, 5'-TCAATGTCAGCATGCACGTA-3').

**Extraction and Analysis of Leaf Protein.** Proteins were extracted from leaf tissues as follows. Eight leaf discs were ground in liquid nitrogen, extracted into 0.4 ml of extraction buffer [20 mM sodium phosphate, pH 7.5; 0.1% (vol/vol) 2-mercapto ethanol; 1% (wt/vol) polypyrrolidone], and filtrated through two layers of miracloth (Calbiochem). Samples corresponding to equal amounts of leaf tissue were loaded onto SDS/PAGE gels. An antiserum raised against LHCII protein of *Festuca pratensis* was used for immunoblot analyses (38).

## Results and Discussion

**Identification of Possible PaO Genes in the *Arabidopsis* Genome.** The PaO/RCCR catalyzed reaction has been extensively characterized in the past (4, 13, 14, 20, 22). Exploiting PaO properties known from these biochemical analyses, we performed an *in silico* analysis to narrow down the number of putative genes in the *Arabidopsis* genome potentially encoding PaO. PaO is a nonheme iron (NHI) containing monoxygenase. *In vitro*, the activity of PaO is independent of a pterin,  $\alpha$ -ketoglutarate, or ascorbate (14), known to be cofactors of different NHI proteins (39). Taken together, this information restricts the molecular nature of PaO to two major types of NHI enzymes, i.e., Rieske- and diiron-oxo-type oxygenases (39). For iron-coordinating clusters of both types of NHI enzymes, conserved motifs have been

established that we used to screen the ATH1.pep database of the *Arabidopsis* Genome Initiative (31). From nine (Rieske) and 4,200 (diiron-oxo) hits obtained, respectively, proteins were selected that met additional properties of PaO, in particular its localization in the chloroplast inner envelope (18). Thus, proteins were selected that contained a putative cTP and putative transmembrane domains (TM). After elimination of proteins containing a putative TM only within the predicted cTP and furthermore of proteins with a predicted pI below 7.0 (envelope proteins generally have a rather alkaline pI; ref. 40), proteins with known function were excluded (Fig. 1B). Among the resulting 21 proteins (Table 1) was Accelerated Cell Death 1 (ACD1, At3g44880) the maize homologue of which Lethal Leaf Spot 1 (LLS1) has been cloned (41).

Although its biochemical function has not been established, *Lls1* was proposed to encode an active suppressor of cell death (41) that plays a role in the removal of a potential photosensitive metabolite (42). ACD1 and its closest relative (At4g25650) occurred in both the Rieske and the diiron-oxo search and appeared to us the most likely candidates for PaO for the following reasons. (i) *lls1* and *acd1* mutants develop a light-dependent lesion mimic phenotype (41–43) that, by analogy to *acd2* mutants (30), might result from the accumulation of intermediates of chl catabolism. (ii) ACD1 and LLS1 are predicted to contain a Rieske-type iron-sulfur cluster and a mononuclear iron-binding site necessary for oxygen activation. (iii) ACD1 has been assigned to the envelope in a plastid proteomic approach (S. Baginsky, personal communication). (iv) Gene expression analyses by using Affymetrix GeneChips demonstrated that *Acd1* gene expression is enhanced during *Arabidopsis* leaf senescence (V. Buchanan-Wollaston and U. Zentgraf, personal communications), and (v) the *Arabidopsis* genome encodes four ACD1-related proteins (42), one of which (At1g44446) is chl *a* oxygenase that catalyses the conversion of chl *a* to *b*. Interestingly, like in the PaO reaction (22), one atom of molecular  $O_2$  is incorporated into the substrate, the electrons being supplied by reduced Fd (24). For these reasons, initial studies focused on ACD1 and its closest relative At4g25650 (Table 1).

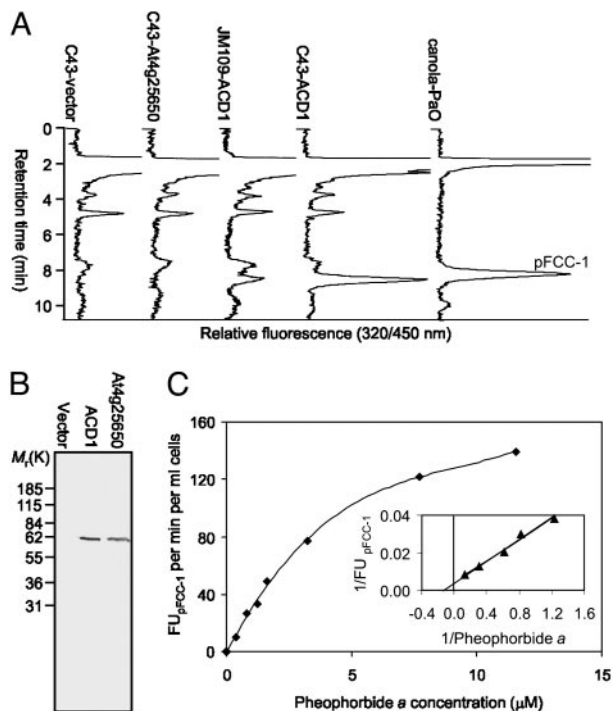


**Fig. 2.** *In vitro* formation of pFCC-1 by using heterologously expressed ACD1 and kinetics of pFCC-1 formation. (A) HPLC traces of PaO/RCCR assays with protein extracts of *E. coli* JM109 or C43, transformed with the expression vector harboring either no insert (C43-vector), At4g25650 cDNA (C43-At4g25650), or ACD1 cDNA (JM109-ACD1 and C43-ACD1, respectively). An assay using PaO from senescent canola cotyledons (canola-PaO) was used as an authentic pFCC-1 standard. (B) Immunoblot analysis of *E. coli* C43 cells transformed with the pQE30 expression vector harboring either no insert (Vector Laboratories), ACD1 cDNA (ACD1), or At4g25650 cDNA (At4g25650). The blot was developed by using an antibody against the His-tag. (C) Nonlinear regression of pFCC-1 formation of C43-ACD1 protein extracts vs. pheide *a* concentration. (Inset) The  $K_m$  value was derived from a Lineweaver–Burk plot.

**Functional Expression of AtPaO/ACD1 in *E. coli*.** To investigate whether ACD1 or At4g25650 has PaO activity, we expressed cDNA sequences of both in two different *E. coli* strains. *In vitro* assays using crude *E. coli* extracts (Fig. 2A) demonstrated that pFCC-1-forming activity was obtained only from cells expressing ACD1. In addition, activity was higher in *E. coli* C43 that exhibits improved capacity for the production of eukaryotic membrane proteins (44). Expression of proteins was confirmed by Western blot analysis by using an antibody directed against the His-tag (Fig. 2B). PaO activity in C43-ACD1 cells exhibited requirements identical to those of PaO activity from senescent canola chloroplasts (14). Thus, pFCC-1 formation required RCCR, Fd, a Fd-reducing system, and the substrates pheide *a* and O<sub>2</sub> (data not shown). pFCC-1 formation as a function of pheide *a* concentrations followed Michaelis–Menten kinetics (Fig. 2C) with an apparent  $K_m$  of 6.0  $\mu$ M. As shown for PaO from canola (14), pheide *b* was not a substrate for heterologously expressed ACD1 (data not shown). In addition, a type 2 RCCR (5) that specifically produces the C1 isomer of pFCC-1 (pFCC-2), together with recombinant PaO, yielded pFCC-2 as well (not shown). Taken together, these data show that ACD1 has PaO activity *in vitro*.

**LLS1 Is Required for chl Breakdown.** To elucidate whether ACD1 and/or its maize homologue LLS1 are responsible for chl catabolism *in vivo* as well, we analyzed an *lls1* mutant in respect to senescence-related characteristics. The lesions of *lls1* have

been described to occur in a development-related fashion (41). Thus, lesion formation mostly starts at the tip of a leaf, with the oldest leaf being affected first. Subsequently, lesions run down the leaf blade progressing from the center to the edges. This phenotype very much resembles senescence progression in wild-type leaves (Fig. 3A). The absence of LLS1 RNA from mutant tissues was confirmed by RT-PCR (Fig. 3B). We analyzed tissues indicated by the boxed areas of Fig. 3A for the presence of green chl catabolites (Fig. 3C). In necrotic mutant tissue, pheide *a* was present at rather high concentrations. No polar chl catabolites accumulated in *lls1* green leaf tissue or in the wild-type tissues. Concomitant with the disappearance of chl in wild type, the appearance of NCCs as the final catabolites of chl was observed (Fig. 3D). To our knowledge, NCCs have so far not been characterized from maize. Deduced from their typical absorbance spectrum (Fig. 3E and ref. 1), there are two NCCs, tentatively named *Zm*-NCC-1 and -2 (for a nomenclature of NCCs, see ref. 36). The structures of these NCCs remain unresolved, but from their retention time on reversed-phase HPLC, they appear to represent unique NCCs not found in other plant species analyzed so far. *Zm*-NCC-1 and -2 did not accumulate in *lls1* (Fig. 3D). Furthermore, we assessed PaO activity in mature green leaf tissues and necrotic and senescent tissue of *lls1* and wild type, respectively. Only extracts from senescent wild-type leaves produced substantial amounts of pFCC-1 in the *in vitro* assay (Fig. 3F).

The obvious correlation of lesion formation in *lls1* with leaf senescence in wild type tempted us to use an artificial system for senescence induction, i.e., dark incubation of excised leaf discs. Under these conditions, chl degradation was retarded in *lls1*, whereas in wild type, chl was degraded in a time-dependent manner (Fig. 4A). NCCs were exclusively found in wild type and their accumulation positively correlated with the loss of chl (data not shown). Again, pheide *a* but not *b* or chlorophyllides progressively accumulated in *lls1* but not in wild type (Fig. 4B). The same result was obtained in preliminary experiments with an *Arabidopsis* line harboring a T-DNA insertion in *Acd1* (data not shown). Two recessive mutants, *F. pratensis* Bf 993 and Mendel’s “green peas,” have been described that accumulate pheide *a* on senescence induction. Although the affected genes have not been identified, in both mutants, absence of PaO activity is the biochemical lesion causing a stay-green phenotype (45, 46). In dark-incubated nonyellowing *lls1* segments, PaO activity was absent as well (data not shown). Activity of PaO has been shown to be senescence-specifically regulated (Fig. 3F and refs. 13, 14); thus, the absence of PaO activity in *lls1* raised the question whether senescence was initiated at all in the mutant. We therefore investigated protein degradation during dark-incubation of leaf discs. Overall protein concentrations decreased similarly in wild type and *lls1* (Fig. 4C), but a chl-binding polypeptide, light-harvesting complex protein II, was specifically retained in *lls1* (Fig. 4D). Again, the same observation had been made in Bf 993 (47), indicating that in the absence of light, *lls1* exhibits a stay-green phenotype, similar to the Bf 993 mutant of *F. pratensis*. Together, the analysis of senescence-related characteristics of *lls1* strongly supports the conclusion that the maize ACD1 orthologue, LLS1, is a PaO that is indispensable for the degradation of chl beyond the level of pheide *a*. We have shown that *Lls1/Acd1* encode PaO enzymes that are involved in senescence-related chl degradation *in vivo*. Therefore, we designate the respective maize and *Arabidopsis* genes *ZmPaO* and *AtPaO*, respectively.

**Both PaO Expression and Activity Are Regulated.** Because of the senescence-related activity of PaO (13, 14), we investigated the expression of *AtPaO/Acd1* during senescence of *Arabidopsis* leaves. Expression levels were normalized to the levels of mRNA encoding the actin 2 protein (48). *Sag12* encoding a senescence-



close relationship between pheide *a* content and ion leakage (data not shown). Thus, in *lls1*, cell death occurred faster when leaf discs had accumulated higher amounts of pheide *a*. This reaction was light-dependent, indicating that photoactivation of pheide *a* may trigger the formation of reactive oxygen species, which in turn cause cell death. This clearly demonstrates that in *lls1*, cell death occurs because of the accumulation of a photo-toxic compound, pheide *a*, rather than because of a direct interference with a cell death suppression mechanism (41). The identification of lesion mimic mutants has been described as a powerful tool to unravel programmed cell death pathways in plants (51). Our finding here, along with the isolation of several lesion mimic mutants in which accumulation of intermediates of chl metabolism causes premature cell death (27, 30), indicates that the relationship between the biochemical function of the respective genes and their involvement in a cell death pathway under wild-type conditions remains a complex puzzle yet to be solved.

The biochemical analysis of heterologously expressed ACD1 and the characteristics of the *lls1* mutant demonstrate that these proteins are identical to PaO, a key enzyme in the catabolism of chl. The wide distribution of *PaO*-like genes within photosynthetic organisms indicates their importance. *PaO*-like genes are present not only in higher plants but also in *Chlamydomonas*

*reinhardtii* (data not shown) and cyanobacteria (42). In contrast, *PaO* is not found (data not shown) in the genome of *Chlorobium tepidum*, an anoxygenic photosynthetic bacterium (52). These bacteria may contain an unrelated oxygen-independent version of PaO. Alternatively, the invention of chl catabolism may have become indispensable for the evolution of oxygenic photosynthetic organisms. This is supported by the finding in several lower plant species of chl degradation products, mainly of the type of RCCs (2, 53, 54). The ability of chl to absorb light and, thus, to enable the conversion of light energy to chemical energy during photosynthesis is vitally important for all life on earth, but it turns into a threat when chl is released from its natural appropriate environment during uncontrolled senescence.

We thank U. Fischer, University of Kaiserslautern, Kaiserslautern, Germany, for support with quantitative RT-PCR analysis; E. Neuhaus for *E. coli* C43 strain; M. Geissler, University of Zurich, Zurich, for antibodies; H. Thomas, H. Ougham and I. Donnison, Institute of Grassland and Environmental Research, Aberystwyth, U.K., for antibodies and discussion; and L. Bovet, U. Feller, E. Martinoia, and P. Matile for support and discussion. Especially, we thank N. Amrhein for critical reading of the manuscript and for discussion. S.H. was supported by grants from the Swiss National Science Foundation; M.R. was supported by a grant from the Spanish Government.

- Kräutler, B., Jaun, B., Bortlik, K.-H., Schellenberg, M. & Matile, P. (1991) *Angew. Chem. Int. Ed. Engl.* **30**, 1315–1318.
- Hörtensteiner, S. (1999) *Cell. Mol. Life Sci.* **56**, 330–347.
- Matile, P., Hörtensteiner, S. & Thomas, H. (1999) *Annu. Rev. Plant Physiol. Plant Mol. Biol.* **50**, 67–95.
- Rodoni, S., Mühlecker, W., Anderl, M., Kräutler, B., Moser, D., Thomas, H., Matile, P. & Hörtensteiner, S. (1997) *Plant Physiol.* **115**, 669–676.
- Hörtensteiner, S., Rodoni, S., Schellenberg, M., Vicentini, F., Nandi, O. I., Qiu, Y.-L. & Matile, P. (2000) *Plant Biol.* **2**, 63–67.
- Kreuz, K., Tommasini, R. & Martinoia, E. (1996) *Plant Physiol.* **111**, 349–353.
- Mühlecker, W., Kräutler, B., Ginsburg, S. & Matile, P. (1993) *Helv. Chim. Acta* **76**, 2976–2980.
- Mühlecker, W. & Kräutler, B. (1996) *Plant Physiol. Biochem.* **34**, 61–75.
- Hinder, B., Schellenberg, M., Rodoni, S., Ginsburg, S., Vogt, E., Martinoia, E., Matile, P. & Hörtensteiner, S. (1996) *J. Biol. Chem.* **271**, 27233–27236.
- Oberhuber, M., Berghold, J., Breuker, K., Hörtensteiner, S. & Kräutler, B. (2003) *Proc. Natl. Acad. Sci. USA* **100**, 6910–6915.
- Takamiya, K., Tsuchiya, T. & Ohta, H. (2000) *Trends Plant Sci.* **5**, 426–431.
- Thomas, H., Ougham, H. & Hörtensteiner, S. (2001) in *Advances in Botanical Research*, ed. Callow, J. A. (Academic, San Diego), Vol. 35, pp. 1–52.
- Ginsburg, S., Schellenberg, M. & Matile, P. (1994) *Plant Physiol.* **105**, 545–554.
- Hörtensteiner, S., Vicentini, F. & Matile, P. (1995) *New Phytol.* **129**, 237–246.
- Trebitsh, T., Goldschmidt, E. E. & Riov, J. (1993) *Proc. Natl. Acad. Sci. USA* **90**, 9441–9445.
- Tsuchiya, T., Ohta, H., Okawa, K., Iwamatsu, A., Shimada, H., Masuda, T. & Takamiya, K. (1999) *Proc. Natl. Acad. Sci. USA* **96**, 15362–15367.
- Rodoni, S., Vicentini, F., Schellenberg, M., Matile, P. & Hörtensteiner, S. (1997) *Plant Physiol.* **115**, 677–682.
- Matile, P. & Schellenberg, M. (1996) *Plant Physiol. Biochem.* **34**, 55–59.
- Schellenberg, M., Matile, P. & Thomas, H. (1993) *Planta* **191**, 417–420.
- Wüthrich, K. L., Bovet, L., Hunziker, P. E., Donnison, I. S. & Hörtensteiner, S. (2000) *Plant J.* **21**, 189–198.
- Frankenberg, N., Mukougawa, K., Kohchi, T. & Lagarias, J. C. (2001) *Plant Cell* **13**, 965–978.
- Hörtensteiner, S., Wüthrich, K. L., Matile, P., Ongania, K.-H. & Kräutler, B. (1998) *J. Biol. Chem.* **273**, 15335–15339.
- Kräutler, B. & Matile, P. (1999) *Acc. Chem. Res.* **32**, 35–43.
- Tanaka, A., Ito, H., Tanaka, R., Tanaka, N. K., Yoshida, K. & Okada, K. (1998) *Proc. Natl. Acad. Sci. USA* **95**, 12719–12723.
- Ito, H., Ohysuka, T. & Tanaka, A. (1996) *J. Biol. Chem.* **271**, 1475–1479.
- Scheumann, V., Schoch, S. & Rüdiger, W. (1999) *Planta* **209**, 364–370.
- Hu, G., Yalpani, N., Briggs, S. P. & Johal, G. S. (1998) *Plant Cell* **10**, 1095–1105.
- Kruse, E., Mock, H.-P. & Grimm, B. (1995) *EMBO J.* **14**, 3712–3720.
- Greenberg, J. T., Guo, A., Klessig, D. F. & Ausubel, F. M. (1994) *Cell* **77**, 551–563.
- Mach, J. M., Castillo, A. R., Hoogstraten, R. & Greenberg, J. T. (2001) *Proc. Natl. Acad. Sci. USA* **98**, 771–776.
- Arabidopsis* Genome Initiative. (2000) *Nature* **408**, 796–813.
- Kurtz, D. M. (1997) *J. Biol. Inorg. Chem.* **2**, 159–167.
- Seki, M., Narusaka, M., Kamiya, A., Ishida, J., Satou, M., Sakurai, T., Nakajima, M., Enju, A., Akiyama, K., Oono, Y., et al. (2002) *Science* **296**, 141–145.
- Lineweaver, H. & Burk, D. (1934) *J. Am. Chem. Soc.* **56**, 658–666.
- Langmeier, M., Ginsburg, S. & Matile, P. (1993) *Physiol. Plant* **89**, 347–353.
- Ginsburg, S. & Matile, P. (1993) *Plant Physiol.* **102**, 521–527.
- Strain, H. H., Cope, B. T. & Svec, W. A. (1971) *Methods Enzymol.* **23**, 452–487.
- Hörtensteiner, S., Chinner, J., Matile, P., Thomas, H. & Donnison, I. S. (2000) *Plant Mol. Biol.* **42**, 439–450.
- Solomon, E. I., Brunold, T. C., Davis, M. I., Kemsley, J. N., Lee, S.-K., Lehnert, N., Neese, F., Skulan, A. J., Yang, Y.-S. & Zhou, J. (2000) *Chem. Rev.* **100**, 235–349.
- Ferro, M., Salvi, D., Rivière-Rolland, H., Verdat, T., Seigneurin-Berny, D., Grunwald, D., Garin, J., Joyard, J. & Rolland, N. (2002) *Proc. Natl. Acad. Sci. USA* **99**, 11487–11492.
- Gray, J., Close, P. S., Briggs, S. P. & Johal, G. S. (1997) *Cell* **89**, 25–31.
- Gray, J., Janick-Buckner, D., Buckner, B., Close, P. S. & Johal, G. S. (2002) *Plant Physiol.* **130**, 1894–1907.
- Greenberg, J. T. & Ausubel, F. M. (1993) *Plant J.* **4**, 327–341.
- Miroux, B. & Walker, J. E. (1996) *J. Mol. Biol.* **260**, 289–298.
- Vicentini, F., Hörtensteiner, S., Schellenberg, M., Thomas, H. & Matile, P. (1995) *New Phytol.* **129**, 247–252.
- Thomas, H., Schellenberg, M., Vicentini, F. & Matile, P. (1996) *Bot. Acta* **109**, 3–4.
- Hilditch, P. I., Thomas, H., Thomas, B. J. & Rogers, L. J. (1989) *Planta* **177**, 265–272.
- Bovet, L., Eggmann, T., Meylan-Bettex, M., Polier, J., Kammer, P., Marin, E., Feller, U. & Martinoia, E. (2003) *Plant Cell Environ.* **26**, 371–381.
- Noh, Y. S. & Amasino, R. M. (1999) *Plant Mol. Biol.* **41**, 181–194.
- Noh, Y. S. & Amasino, R. M. (1999) *Plant Mol. Biol.* **41**, 195–206.
- Lorrain, S., Vaillieu, F., Balagué, C. & Roby, D. (2003) *Trends Plant Sci.* **8**, 263–271.
- Eisen, J. A., Nelson, K. E., Paulsen, I. T., Heidelberg, J. F., Wu, M., Dodson, R. J., Deboy, R., Gwinn, M. L., Nelson, W. C., Haft, D. H., et al. (2002) *Proc. Natl. Acad. Sci. USA* **99**, 9509–9514.
- Engel, N., Jenny, T. A., Mooser, V. & Gossauer, A. (1991) *FEBS Lett.* **293**, 131–133.
- Doi, M., Shima, S., Egashira, T., Nakamura, K. & Okayama, S. (1997) *J. Plant Physiol.* **150**, 504–508.